Chapter 2
Inviscid, Incompressible Flow Past Circular Cylinders and Joukowski Airfoils

2.1 Background

2.1.1 Notation

In two-dimensions, the obstacles are cylinders of various cross sections, whose axis is perpendicular to the plane in which the flow is taking place (Fig. 2.1). When a wing will be considered, the wing span will be described by the variable y. Hence, the flow past cylinders will take place in the (x, z) plane, see Fig. 2.2. In this chapter we will consider steady, 2-D, inviscid, incompressible, adiabatic and irrotational flow, also called *potential flow*. The influence of gravity will be neglected.

2.1.2 Governing Equations

Lets (u, w) represent the perturbation velocity or deviation from the uniform flow $\mathbf{V}_\infty = (U, 0)$. At any point in the flow field the velocity is $\mathbf{V} = (U + u, w)$, the density is $\rho = const.$ and the pressure p. The conservation of mass and irrotationality condition form a system of two linear first-order partial differential equations (PDEs) for (u, w) as

$$\begin{cases} \frac{\partial u}{\partial x} + \frac{\partial w}{\partial z} = 0 \\ \frac{\partial u}{\partial z} - \frac{\partial w}{\partial x} = 0 \end{cases} \tag{2.1}$$

In local polar coordinates (r, θ), the system reads in terms of $\mathbf{V} = (V_r, V_\theta)$

$$\begin{cases} \frac{\partial r v_r}{\partial r} + \frac{\partial v_\theta}{\partial \theta} = 0 \\ \frac{\partial r v_\theta}{\partial r} - \frac{\partial v_r}{\partial \theta} = 0 \end{cases} \tag{2.2}$$

J.J. Chattot and M.M. Hafez, *Theoretical and Applied Aerodynamics*,
DOI 10.1007/978-94-017-9825-9_2

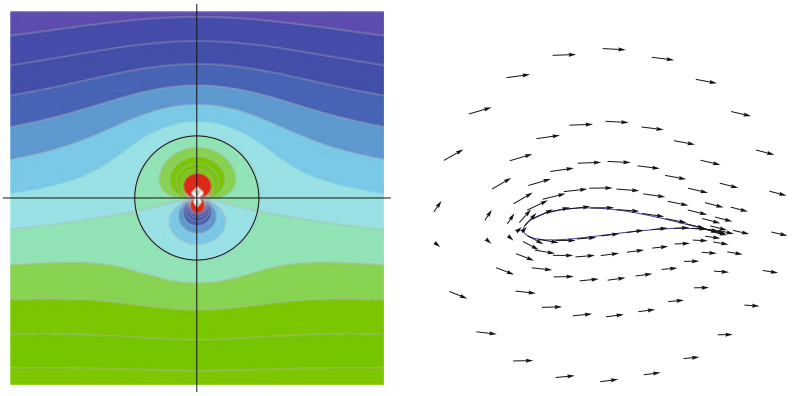

Fig. 2.1 Flow past a circular cylinder with circulation and mapping to a Joukowski airfoil

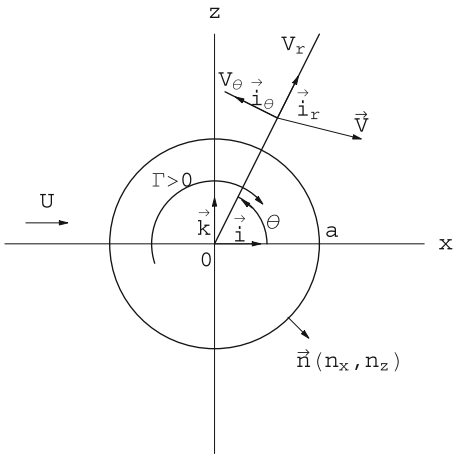

Fig. 2.2 Coordinate system and notation

where $V_r = U\cos\theta + v_r$ and $V_\theta = -U\sin\theta + v_\theta$ are the total velocity components, including the contribution of the uniform flow. The irrotationality condition is the consequence of conservation of momentum for inviscid, adiabatic, incompressible flow. In other words, a solution to the above system also satisfies the momentum equations. The energy equation (conservation of mechanical energy) is also satisfied, under the stated assumptions.

The pressure is obtained from Bernoulli's equation, again a consequence of the momentum conservation (it can be interpreted also as a conservation of mechanical energy per unit mass, where the potential energy is constant):

$$\frac{p}{\rho} + \frac{1}{2}V^2 = \frac{p_\infty}{\rho} + \frac{1}{2}\mathbf{V}_\infty^2 = \frac{p_\infty}{\rho} + \frac{1}{2}U^2 = const. \tag{2.3}$$

Note that the Bernoulli's equation is nonlinear. However, as we will see, it can be linearized under the assumption of small perturbation.

2.1.3 Boundary Conditions

The boundary conditions determine the solution of the PDEs. They correspond to the necessary and sufficient conditions for the well-posedness of solutions to the PDEs, i.e. to exist, be unique and depend continuously on the data. There are two types of boundary conditions traditionally associated with the above system, the tangency condition and the asymptotic condition in the far field.

The tangency condition expresses the fact that in an inviscid flow, the fluid is expected to slip along a solid, impermeable surface. This translates to

$$(\mathbf{V}.\mathbf{n})_{obstacle} = V_n = 0 \tag{2.4}$$

where V_n represents the normal relative velocity with respect to the solid surface.

Other conditions can be prescribed, for example in the case of a porous surface, the normal relative velocity can be given as

$$V_n = g \tag{2.5}$$

where g is a given function along the surface.

The asymptotic condition states that, for a finite obstacle, the flow far away from the body, returns to the uniform, undisturbed flow $\mathbf{V}_\infty$. In terms of u and w this reads

$$u, w \to 0 \; as \; x^2 + z^2 \to \infty \tag{2.6}$$

2.1.4 Other Formulations

For irrotational flows, a velocity potential can be introduced: let $\phi(x, z)$ be the perturbation potential. The full potential is given by $\Phi = Ux + \phi(x, z)$. The perturbation velocity components are

$$u = \frac{\partial \phi}{\partial x}, \; w = \frac{\partial \phi}{\partial z} \tag{2.7}$$

Then the irrotationality condition is identically satisfied, but substituting u and w into the conservation of mass results in

$$\Delta\phi = \frac{\partial^2 \phi}{\partial x^2} + \frac{\partial^2 \phi}{\partial z^2} = 0 \tag{2.8}$$

In polar coordinates this is

$$v_\theta = \frac{1}{r}\frac{\partial \phi}{\partial \theta},\ v_r = \frac{\partial \phi}{\partial r} \tag{2.9}$$

$$\frac{\partial}{\partial r}\left(r\frac{\partial \phi}{\partial r}\right) + \frac{1}{r}\frac{\partial^2 \phi}{\partial \theta^2} = 0 \tag{2.10}$$

This is the governing equation for potential flows, the Laplace equation. The perturbation velocity field is given by $grad\ \phi = \left(\frac{\partial \phi}{\partial x}, \frac{\partial \phi}{\partial y}, \frac{\partial \phi}{\partial z}\right)$ (or in short notation $\nabla\phi$). The boundary conditions become

$$\begin{cases} \nabla \Phi.\mathbf{n}\,|_{obstacle} = (U\mathbf{i} + \nabla\phi).\mathbf{n}\,|_{obstacle} = 0 \\ \nabla\phi \to 0\ as\ x^2 + z^2 \to \infty \end{cases} \tag{2.11}$$

A streamfunction can be introduced: let $\psi(x, z)$ be the perturbation streamfunction. The full stream function is $\Psi = Uz + \psi(x, z)$. The perturbation velocity components are obtained from

$$u = \frac{\partial \psi}{\partial z},\ w = -\frac{\partial \psi}{\partial x} \tag{2.12}$$

then the equation of conservation of mass is identically satisfied and substituting u and w in the irrotationality condition yields

$$\Delta\psi = \frac{\partial^2 \psi}{\partial x^2} + \frac{\partial^2 \psi}{\partial z^2} = 0 \tag{2.13}$$

In polar coordinates this is also

$$v_r = \frac{1}{r}\frac{\partial \psi}{\partial \theta},\ v_\theta = -\frac{\partial \psi}{\partial r} \tag{2.14}$$

$$\frac{\partial}{\partial r}\left(r\frac{\partial \psi}{\partial r}\right) + \frac{1}{r}\frac{\partial^2 \psi}{\partial \theta^2} = 0 \tag{2.15}$$

This is the governing equation for the streamfunction. The streamfunction also satisfies Laplace equation. The boundary conditions, however, read

$$\begin{cases} \Psi\,|_{obstacle} = (Uz + \psi)\,|_{obstacle} = const. \\ \left(\frac{\partial \psi}{\partial z}, -\frac{\partial \psi}{\partial x}\right) \to 0\ as\ x^2 + z^2 \to \infty \end{cases} \tag{2.16}$$

The first condition results from the identity $\nabla\Psi.\mathbf{t}|_{obstacle} = 0$, where $\mathbf{t}$ represents a unit tangent vector to the solid surface ($\mathbf{n}.\mathbf{t} = 0$), which proves that $\Psi\,|_{obstacle} = const.$, the value of this constant is however not known a priori. The

$\Psi = const.$ lines are the streamlines of the flow. Solid obstacles are streamlines and conversely, streamlines can be materialized to represent a body surface.

When both, Φ and Ψ exist, simultaneously, potential and stream functions are called conjugate harmonic functions. It can be easily shown that the curves $\Phi = const.$ are orthogonal to the curves $\Psi = const.$

2.2 Elementary Solutions

2.2.1 Uniform Flow

The uniform flow $\mathbf{V}_\infty = (U, 0)$ is represented by the leading term of the full potential and stream functions:

$$\Phi = Ux, \ \Psi = Uz \tag{2.17}$$

A sketch of the solution is shown in Fig. 2.3.

The uniform flow $\mathbf{W}_\infty = (0, W)$ is represented by the leading term of the full potential and stream functions:

$$\Phi = Wz, \ \Psi = -Wx \tag{2.18}$$

A sketch of the solution is shown in Fig. 2.4.

A uniform flow in an arbitrary direction can be obtained by the superposition of these two elementary solutions.

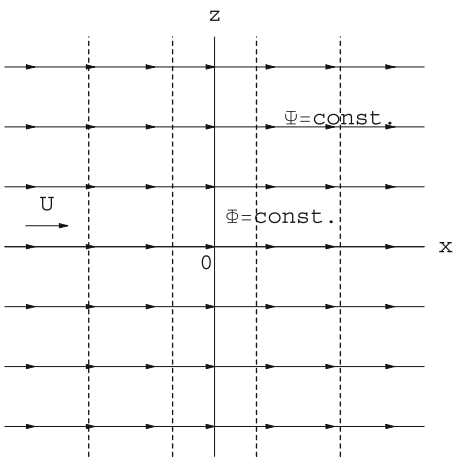

Fig. 2.3 Uniform flow: equipotential lines and streamlines

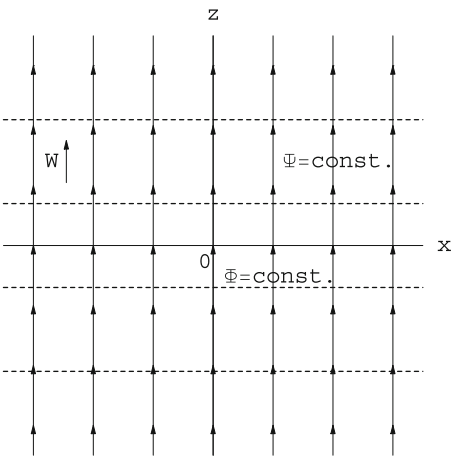

Fig. 2.4 Uniform flow: equipotential lines and streamlines

2.2.2 Source and Sink

A line source and sink is the building block to represent profile thickness as will be seen later. If a source or a sink is placed in the plane, it is convenient to define a polar coordinate system with origin at the source or sink location. Let (r, θ) represent the distance and polar angle of a point to the source/sink.

The velocity components are

$$v_r = \frac{Q}{2\pi}\frac{1}{r}, \; v_\theta = 0 \tag{2.19}$$

Note that the perturbation velocity vanishes in the far field, which is consistent with the asymptotic condition. The potential and stream functions are given by

$$\phi = \frac{Q}{2\pi}\ln r, \; \psi = \frac{Q}{2\pi}\theta \tag{2.20}$$

Q represents the source/sink intensity and has unit of volume flow rate per unit span (m^2/s). $Q > 0$ is a source, $Q < 0$ a sink. The equipotential lines are circles and the streamlines are rays through the origin. See Fig. 2.5.

2.2.3 Doublet

A doublet is obtained when a source $(Q, -a)$ and a sink $(-Q, a)$ located symmetrically along the x-axis are merged at the origin following the limiting process

$$lim_{a\to 0,\; Q\to\infty}\,(Source(Q, -a) + Sink(-Q, a)) \tag{2.21}$$

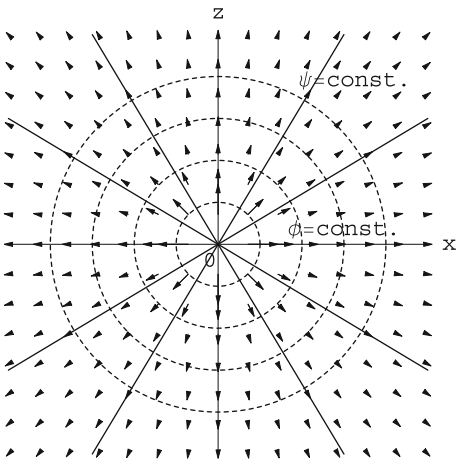

Fig. 2.5 Source: equipotental lines and streamlines

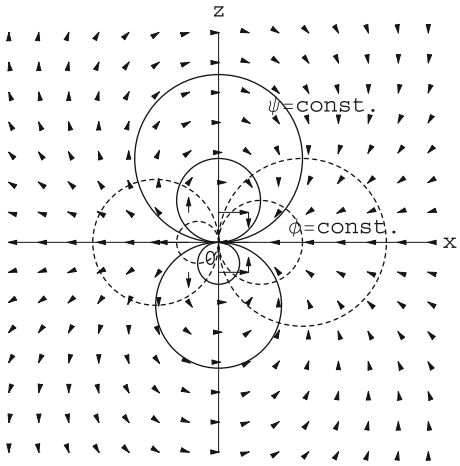

Fig. 2.6 Doublet: equipotential lines and streamlines

The results for the velocity components are

$$v_r = \frac{-D\cos\theta}{r^2},\ v_\theta = \frac{-D\sin\theta}{r^2} \tag{2.22}$$

where D is the strength of the doublet, $D = lim_{a\to 0,\ Q\to\infty}\, aQ$

The results for the potential and stream functions are

$$\phi = D\frac{\cos\theta}{r},\ \psi = -D\frac{\sin\theta}{r} \tag{2.23}$$

The equipotential lines and streamlines are circles, tangent at the origin to the z-axis for the former and to the x-axis for the latter. See Fig. 2.6.

2.2.4 Potential Vortex

Consider a cylinder rotating clockwise in a fluid at rest at infinity. The particles will be entrained, through viscous shear forces, to move around the cylinder in concentric circles. It can be shown that, at steady-state, such a flow is irrotational and the velocity is given by

$$v_r = 0,\ 2\pi r v_\theta = const. = -\Gamma \tag{2.24}$$

Γ is called the vortex strength or circulation and has unit (m^2/s). Such a potential flow around the cylinder is called a potential vortex (this terminology may be confusing since the vorticity in such a flow is zero outside the cylinder otherwise it is not a potential flow). Now, the cylinder radius can be vanishingly small. The potential flow solution however is singular at $r = 0$, a point inside the cylinder, no matter how small the radius is.

Notice that a potential vortex corresponds to the flow obtained when the potential and stream lines of a source/sink flow are exchanged. The solution is given by

$$\phi = -\frac{\Gamma}{2\pi}\theta,\ \psi = \frac{\Gamma}{2\pi}\ln r \tag{2.25}$$

The potential lines are now the rays and the streamlines the circles centered at the origin. See Fig. 2.7. The vortex solution is a building block for lifting airfoils to represent incidence and camber as will be seen later.

Note that the velocity components (u, w) (obtained from ϕ and ψ by taking the partial derivatives with respect to x and z when using the Cartesian coordinates, or $\frac{\partial}{\partial r}$ and $\frac{1}{r}\frac{\partial}{\partial \theta}$ when using polar coordinates), decay in the far field as $\frac{1}{r}$, which is consistent with the asymptotic condition.

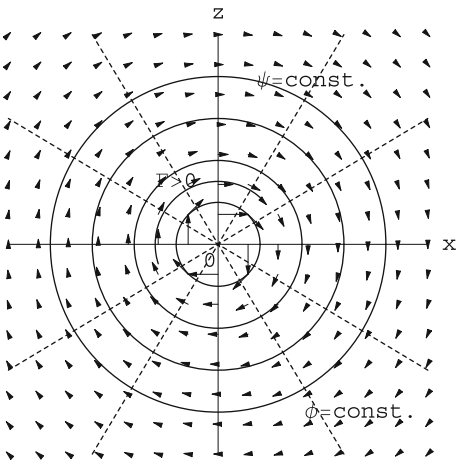

Fig. 2.7 Potential vortex: potential lines and streamlines

2.3 Superposition of Elementary Solutions

From the property of linear governing equations, if ϕ_1 and ϕ_2 are each solution of the Laplace equation, $\phi_1 + \phi_2$ or any linear combination will be a solution of the Laplace equation. The same is true for the stream functions. This is the basis of the principle of superposition. Note that the elementary solutions for ϕ and ψ are singular at their centers (infinite velocity), hence they are also called singular solutions and the superposition of singular solutions is called the method of singularities. These singular solutions are regular everywhere in the flow field when the centers are excluded, for example by enclosing them within the obstacle.

Mathematically one can prove that it is possible to solve for the flow past an arbitrary obstacle by superposing elementary solutions, but, in general, the resulting pressure field is not the sum of the individual pressure fields, due to the nonlinearity of Bernoulli's equation. For small disturbances, the Bernoulli equation can be linearized, allowing for superposition of pressure fields as well.

2.3.1 Global Integrals

Let $Q = \oint_C (\mathbf{V}.\mathbf{n})dl$ and $\Gamma = \oint_C (\mathbf{V}.\mathbf{dl})$, where **dl** represents a small oriented element of the contour and $dl = |\mathbf{dl}|$ is the length of the element. The first integral represents the net volume flow rate out of contour C and the second, the circulation along the same contour, taken in the clockwise direction. It is easy to show that if the contour C contains sources and sinks of intensity $Q_1, Q_2, \ldots$ the result will be $Q = Q_1 + Q_2 + \cdots$ the algebraic sum of the sources and sinks inside the contour. If the contour C contains potential vortices of circulation $\Gamma_1, \Gamma_2, \ldots$ the result will be $\Gamma = \Gamma_1 + \Gamma_2 + \cdots$ the algebraic sum of vortices inside the contour.

2.3.2 Example of Superposition: Semi-infinite Obstacle

The superposition of the uniform flow and a source ($Q > 0$) at the origin produces a semi-infinite body, called Rankine body. Stagnation points and stagnation streamlines play an important role in the description of the flow topology. Here, the velocity field is given by

$$V_r = U\cos\theta + \frac{Q}{2\pi}\frac{1}{r},\ V_\theta = -U\sin\theta \tag{2.26}$$

At a stagnation point $V_r = V_\theta = 0$. The stagnation point S for this flow is found to be

$$\theta_s = \pi,\ r_s = \frac{Q}{2\pi U} \tag{2.27}$$

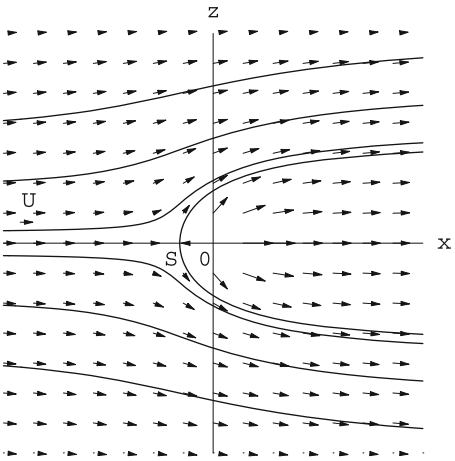

Fig. 2.8 Half-body and flow vector field

The main flow features can be studied with the streamfunction

$$\Psi = Ur\sin\theta + \frac{Q}{2\pi}\theta \tag{2.28}$$

A remarkable streamline is that which corresponds to the half-body. It corresponds to $\Psi = \frac{Q}{2}$. It is also the stagnation streamline. It is made of several pieces, the negative x-axis and the half-body itself. The flow is sketched in Fig. 2.8.

Note that any streamline can be materialized as a solid surface. The flow inside the half body is also represented, however it is singular at the origin and cannot represent a realistic flow near that point. The maximum thickness of the half-body is $\frac{Q}{\pi U}$. One can calculate the force on a solid surface coinciding with the separation streamline using the momentum theorem and Bernoulli's equation applied to a contour composed of the half-body and a large circle of radius R to close the contour. The lift vanishes due to symmetry, but the axial force on the half-body is given by $D = -\rho U Q$, a thrust.

2.4 Flow Past a Circular Cylinder

Finite bodies require that the sum of all sources and sinks be zero. Doublets, as limit of a source and a sink of equal and opposite intensity, have zero net volume flow. The superposition of a uniform flow and a doublet ($D > 0$) produces a flow field given by

$$V_r = U\cos\theta - D\frac{\cos\theta}{r^2},\ V_\theta = -U\sin\theta - D\frac{\sin\theta}{r^2} \tag{2.29}$$

The velocity potential and streamfunction are

$$\Phi = Ur\cos\theta + D\frac{\cos\theta}{r} = \left(Ur + \frac{D}{r}\right)\cos\theta \tag{2.30}$$

$$\Psi = Ur\sin\theta - D\frac{\sin\theta}{r} = \left(Ur - \frac{D}{r}\right)\sin\theta \tag{2.31}$$

By inspection of the streamfunction, one can see that $\Psi = 0$ for $r = a = \sqrt{\frac{D}{U}}$. This solution represents the flow past a circular cylinder of radius a. At the surface of the cylinder, the tangency condition, $V_r = 0$, is satisfied. We have also seen earlier that the potential vortex admits streamlines which are circles centered at the origin. In fact, the most general solution of the flow past a circular cylinder of radius a is given by the superposition of the uniform flow, a doublet of intensity $D = Ua^2$ and a potential vortex. The corresponding velocity field is

$$V_r = U\left(1 - \frac{a^2}{r^2}\right)\cos\theta,\ \ V_\theta = -U\left(1 + \frac{a^2}{r^2}\right)\sin\theta - \frac{\Gamma}{2\pi}\frac{1}{r} \tag{2.32}$$

Note that the circulation Γ is arbitrary. The tangency condition is satisfied by $V_r(a,\theta) = 0$. The asymptotic condition is also satisfied as $\mathbf{V} \to \mathbf{V}_\infty$ when $r \to \infty$.

Stagnation points are found on the cylinder by satisfying the condition

$$V_\theta(a,\theta_s) = -2U\sin\theta_s - \frac{\Gamma}{2\pi}\frac{1}{a} = 0 \tag{2.33}$$

This admits two solutions provided $|\Gamma| \le 4\pi Ua$, namely $\theta_s = \arcsin\left(-\frac{\Gamma}{4\pi Ua}\right)$ and $\pi + \arcsin\left(\frac{\Gamma}{4\pi Ua}\right)$, where $-\frac{\pi}{2} \le \theta_s \le \frac{\pi}{2}$. The stagnation points are points A and B in Fig. 2.9. The streamlines are given by

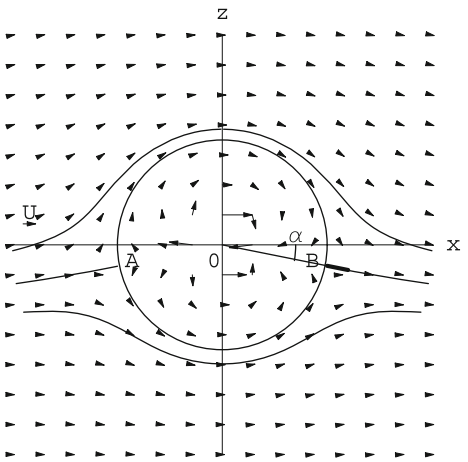

Fig. 2.9 Flow past a circular cylinder with circulation

$$\Psi = U\left(r - \frac{a^2}{r}\right)\sin\theta + \frac{\Gamma}{2\pi}\ln r = const. \tag{2.34}$$

A remarkable streamline is the stagnation streamline, $\Psi = \frac{\Gamma a}{2\pi}$. It is made of the cylinder and the two branches attached to the stagnation points.

The question of how to determine the value for Γ is important. Within the inviscid flow framework, a possible mechanism for controlling the circulation is the use of a small flap, a thin flat plate placed perpendicular to the cylinder at θ_s forcing the rear stagnation point to locate at point B, as shown in Fig. 2.9. Once the rear stagnation point is established, the front stagnation point A will settle at $\pi - \theta_s$. In a sense, θ_s relates to the "incidence" $\alpha = -\theta_s$ of the cylinder. The previous equation for the stagnation points can be written as

$$\Gamma(\alpha) = 4\pi U a \sin\alpha \tag{2.35}$$

which reflects the dependency of the circulation on the flap location.

The pressure field is obtained from the Bernoulli equation

$$p(r,\theta) = p_\infty + \frac{1}{2}\rho(U^2 - V_r^2 - V_\theta^2) \tag{2.36}$$

On the cylinder surface this reduces to

$$p(\theta) = p_\infty + \frac{1}{2}\rho\left[U^2 - \left(\frac{\Gamma}{2\pi a}\right)^2 - \frac{2U\Gamma}{\pi a}\sin\theta - 4U^2\sin^2\theta\right] \tag{2.37}$$

Knowing the surface pressure distribution, one can calculate the lift and drag over the cylinder

$$L' = -\int_0^{2\pi}(p(\theta) - p_\infty)\sin\theta a d\theta,\quad D' = -\int_0^{2\pi}(p(\theta) - p_\infty)\cos\theta a d\theta \tag{2.38}$$

Substituting for $p(\theta)$ in the above formulae yields $L' = \rho U\Gamma$ and $D' = 0$, the latter being an obvious consequence of symmetry.

Another, more practical means of controlling the circulation is by giving the cylinder a rotational speed Ω. Any real fluid having viscosity, the particles in contact with the cylinder will rotate at speed Ω, thus entraining the nearby particles through viscous shear forces to rotate also. As a result, a circulatory flow is created. The relationship between the rotation speed Ω and the circulation Γ is not straightforward, but can be studied numerically or experimentally. See for example the discussion, in the book by White [1], of the Magnus effect and the application to the Flettner rotor ship where the sails are replaced by rotating cylinders. According to Wikipedia (http://en.wikipedia.org): "Assisted by Albert Betz,

Fig. 2.10 Buckau Flettner rotor ship (from https://en.wikipedia.org/wiki/File:Buckau_Flettner_Rotor_Ship_LOC_37764u.jpg)

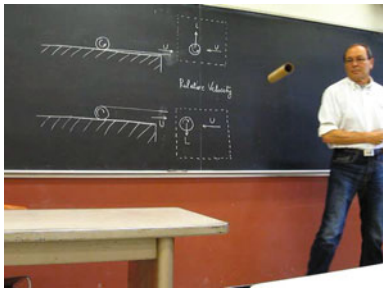

Fig. 2.11 JJC demonstrating the Magnus effect

Jacob Ackeret and Ludwig Prandtl, Flettner constructed an experimental rotor vessel, and in October 1924 the Germaniawerft finished construction of a large two-rotor ship named Buckau. The vessel was a refitted schooner which carried two cylinders (or rotors) about 15 m (50 ft) high, and 3 m (10 ft) in diameter, driven by an electric propulsion system of 50 hp (37 kW) power," Fig. 2.10.

A simple experiment with a small cardboard cylinder and the flat surface of a table demonstrates the Magnus effect. A small string is wound around the cylinder and its extremity is pulled briskly to accelerate the cylinder both in translation and rotation. Depending on the sense of rotation, the cylinder will fall quickly to the ground, or fly for a short time well above the table, see Fig. 2.11.

2.5 Flow Past Arbitrary Airfoils

2.5.1 Kutta-Joukowski Lift Theorem

The theory of conformal mapping tells us that it is possible to map any simply connected profile onto a circular cylinder. In the transformation, the flow past the profile maps into the flow past a circular cylinder derived earlier. The far field flow is preserved. The inverse transformation will therefore describe the exact solution of the flow past the original profile. One such transformation is the Joukowski transformation

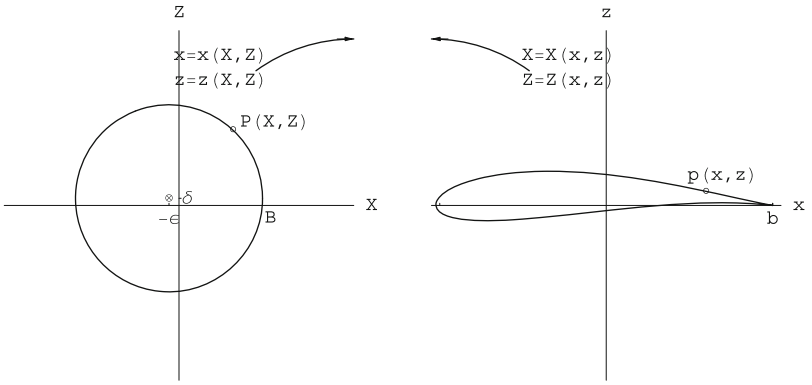

Fig. 2.12 Cylinder plane (X, Z) and physical plane (x, z)

$$x = X\left(1 + \frac{a^2}{X^2 + Z^2}\right), \; z = Z\left(1 - \frac{a^2}{X^2 + Z^2}\right) \tag{2.39}$$

where (x, z) represent the physical plane of the profile and (X, Z) the plane of the cylinder. Notice that the transformation preserves the far field (i.e. $x \to X$ and $z \to Z$ far from the origin). A cylinder of radius r_0, where $r_0^2 = (a + \epsilon)^2 + \delta^2$ centered at $X = -\epsilon$, $Z = \delta$ and passing through point B located at $X = a$, $Z = 0$ maps onto a family of Joukowski airfoils depending on ϵ and δ. The profile has a cusp at the trailing edge, point b, image of point B. See Fig. 2.12. In the figure, p is the image of P through the transformation.

The polar coordinate representation of the cylinder is

$$X = r(\theta)\cos\theta, \; Z = r(\theta)\sin\theta \tag{2.40}$$

where $r(\theta) = -(\epsilon\cos\theta - \delta\sin\theta) + \sqrt{a^2 + 2\epsilon a + (\epsilon\cos\theta - \delta\sin\theta)^2}$.

Through the mapping, the parametric representation of the Joukowski profile is obtained

$$\begin{cases} x(\theta) = \left(r(\theta) + \frac{a^2}{r(\theta)}\right)\cos\theta \\ z(\theta) = \left(r(\theta) - \frac{a^2}{r(\theta)}\right)\sin\theta \end{cases} \tag{2.41}$$

In the mapping, the doublet and potential vortex contribute to a distribution of singularities (sources, sinks and vorticity distributions) inside the profile. In the far field, however, the leading terms in the perturbation velocity field correspond again to a doublet (closed obstacle) and a potential vortex with the same net circulation Γ. To calculate the force on an arbitrary profile, one can apply the momentum theorem to the domain inside a large circle C of radius R centered at the origin

$$\mathbf{F}' = -\oint_C \left[\rho\mathbf{V}(\mathbf{V}.\mathbf{n}) + p\mathbf{n}\right] R d\theta \tag{2.42}$$

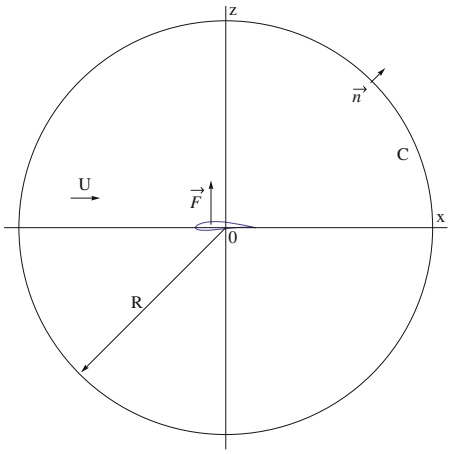

Fig. 2.13 Control surface for application of the momentum theorem

where $\mathbf{F}'$ represents the force per unit span applied by the fluid to the profile. See Fig. 2.13.

We will assume that any solution near C can be expanded asymptotically as

$$v_r = U\cos\theta + O\left(\frac{1}{R^2}\right),\ v_\theta = -U\sin\theta - \frac{\Gamma}{2\pi R} + O\left(\frac{1}{R^2}\right) \tag{2.43}$$

Let $\mathbf{n} = (\cos\theta, \sin\theta)$ then

$$\mathbf{V}.\mathbf{n} = v_r = U\left(1 - \frac{a^2}{R^2}\right)\cos\theta = U\cos\theta + O\left(\frac{1}{R^2}\right) \tag{2.44}$$

The force will be evaluated in the Cartesian coordinate system. The Cartesian form of $\mathbf{V}$ is

$$\mathbf{V} = \left(U + \frac{\Gamma}{2\pi R}\sin\theta + O\left(\frac{1}{R^2}\right)\right)\mathbf{i} + \left(-\frac{\Gamma}{2\pi R}\cos\theta + O\left(\frac{1}{R^2}\right)\right)\mathbf{k} \tag{2.45}$$

where $\mathbf{i}$ and $\mathbf{k}$ are the unit vectors of the x and z-axis respectively. Hence, the first term in the integrand Eq. (2.42) reads

$$\rho\mathbf{V}(\mathbf{V}.\mathbf{n}) = \rho\left[\left(U + \frac{\Gamma}{2\pi R}\sin\theta + O\left(\frac{1}{R^2}\right)\right)\mathbf{i} + \left(-\frac{\Gamma}{2\pi R}\cos\theta + O\left(\frac{1}{R^2}\right)\right)\mathbf{k}\right] \times \left(U\cos\theta + O\left(\frac{1}{R^2}\right)\right) \tag{2.46}$$

When integrated on the circle, the $\cos\theta$ and $\sin\theta\cos\theta$ terms vanish and there remains only

$$\oint_C \rho\mathbf{V}(\mathbf{V}.\mathbf{n})Rd\theta = \oint_C \rho\left[O\left(\frac{1}{R}\right)\mathbf{i} + \left(-\frac{U\Gamma}{2\pi}\cos^2\theta + O\left(\frac{1}{R}\right)\right)\mathbf{k}\right]d\theta \quad (2.47)$$

The pressure term can also be expanded as

$$p(R,\theta) = p_\infty - \frac{1}{2}\rho\left(\frac{\Gamma}{2\pi R}\right)^2 - \frac{\rho U\Gamma}{2\pi R}\sin\theta + O\left(\frac{1}{R^2}\right) \quad (2.48)$$

The first two terms which are constant on the circle vanish in the integration and there remains for the second term in the momentum integral

$$\oint_C \left[-\frac{\rho U\Gamma}{2\pi R}\sin\theta + O\left(\frac{1}{R^2}\right)\right](\cos\theta\mathbf{i} + \sin\theta\mathbf{k})\,Rd\theta \quad (2.49)$$

Again, the product $\sin\theta\cos\theta$ vanishes in the integration and we are left with

$$\oint_C p\mathbf{n}Rd\theta = \oint_C \left[O\left(\frac{1}{R}\right)\mathbf{i} + \left(-\frac{\rho U\Gamma}{2\pi}\sin^2\theta + O\left(\frac{1}{R}\right)\right)\mathbf{k}\right] \quad (2.50)$$

The results is

$$\mathbf{F}' = O\left(\frac{1}{R}\right)\mathbf{i} + \left(\rho U\Gamma + O\left(\frac{1}{R}\right)\right)\mathbf{k} \quad (2.51)$$

Now letting $R \to \infty$ yields the final result

$$\mathbf{F}' = \rho U\Gamma\mathbf{k} \quad (2.52)$$

This result is known as the Kutta-Joukowski lift theorem:

A uniform flow produces on a cylinder of arbitrary cross-section a lift force per unit span $L' = \rho U\Gamma$ that is proportional to the circulation Γ around the profile. The orientation of the force is obtained by rotating the incoming flow velocity vector 90° opposite to the circulation.

Another way to derive this theorem is to consider a control volume as in Fig. 2.14.

If the top and bottom boundaries of the control volume are far from the obstacle (distance H), the pressure will have the atmospheric value and the velocity will be the undisturbed velocity. The circulation, however, will not vanish as it remains constant over any closed curve enclosing the obstacle. The momentum theorem, Eq. (2.42), in projection on the z-axis reduces to

$$L' = -\int_{-\infty}^{\infty} \rho\left([(U+u)w]_{in} - [(U+u)w]_{out}\right)dz \quad (2.53)$$

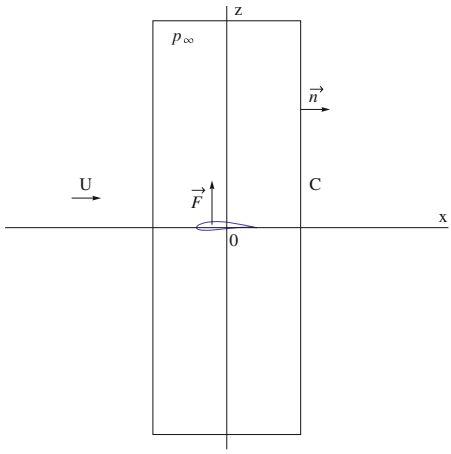

Fig. 2.14 Control volume for the evaluation of lift

where pressure does not contribute because it is atmospheric on the upper and lower surfaces and its action is perpendicular to the z-axis along the side boundaries. Since u and w are of order $O\left(\frac{1}{\sqrt{D^2+H^2}}\right)$ or higher, where D ($H \gg D$) is the distance of the side boundaries to the z-axis, the result can be expressed as

$$L' = \rho U \Gamma + O\left(\frac{H}{D^2 + H^2}\right) \tag{2.54}$$

The final result is obtained by letting $D \to \infty$. A similar approach, with a control volume where now $D \gg H$ can be used to prove that the drag $D' = 0$. This result is consistent with the calculation of the lift over the cylinder, since with the Joukowski transformation or any transformation of the obstacle to a cylinder that preserves the far field, the lift over the obstacle is the same as the lift over the cylinder at the same angle of incidence. Furthermore, as a consequence of the conservation of momentum, the lift is proportional to the circulation as $L' = \rho U \Gamma$ and the drag $D' = 0$.

2.5.2 The d'Alembert Paradox

The d'Alembert paradox results from the fact that when a profile is moving at uniform velocity in a fluid, the resulting force is perpendicular to the velocity. The drag is zero. This result is consistent with the inviscid, frictionless fluid assumption. But in fact, with all real fluids, there is friction along the surface of the profile and there will be (a small) drag. The analysis of viscous forces in the boundary layer will resolve this paradox.

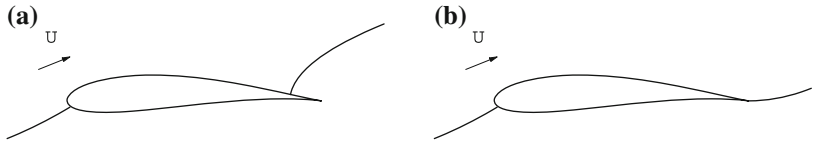

Fig. 2.15 **a** Profile that does not satisfy the K-J condition and **b** Profile that does satisfy the K-J condition

2.6 The Kutta-Joukowski Condition

With the Joukowski transformation, the mapping of the cylinder to the profile is singular at B, $X = a$, $Z = 0$ (the other singular point is at $X = -a$, $Z = 0$). This point corresponds to the cusped trailing edge B of the Joukowski profile, see Fig. 2.12. It has been found experimentally that the flow will leave the profile at a sharp trailing edge (cusp or small angle). This is due to viscosity. As the boundary layer grows from the leading edge to the trailing edge, the fluid particles do not have enough momentum to come around the trailing edge, and hence separate from the profile there. The sharp trailing edge of the profile plays the same role as the flap for the cylinder. This condition makes the inviscid flow solution past a profile unique by fixing the circulation.

The Kutta-Joukowski (K-J) condition states the the flow must leave the profile at the sharp trailing edge "smoothly". See Fig. 2.15.

Revisiting the Joukowski transformation of Sect. 2.5.1, one can see that with an incoming flow making an angle α with the X-axis and with an arbitrary circulation around the cylinder, the rear stagnation point will be located at an arbitrary point such as P in Fig. 2.12, therefore the stagnation streamline will leave the profile at point p and the K-J condition will not be satisfied. The velocity will be infinite at the trailing edge. In order to enforce the K-J condition, the circulation must be adjusted such that the rear stagnation point is located at point B. This uniquely determines the value of the circulation Γ as a function of incidence α.

2.7 Definitions

The chord c of a profile is the radius of the largest circle centered at the trailing edge and touching the leading edge.

The incidence angle or angle of attack is defined as the angle between the profile chord and the incoming flow velocity vector.

It is convenient to use dimensionless coefficients to represent pressure, forces and moments. The pressure coefficient is defined as

$$C_p = \frac{p - p_\infty}{\frac{1}{2}\rho V_\infty^2} = 1 - \left(\frac{V}{V_\infty}\right)^2 \tag{2.55}$$

where the denominator, $\frac{1}{2}\rho V_\infty^2$ is called the dynamic pressure (has dimension of a pressure, unit Pa) and use has been made of the Bernoulli equation.

The lift, drag and moment coefficients per unit span are made dimensionless, in 2-D flow, with the dynamic pressure and a reference length or length squared as

$$C_l = \frac{L'}{\frac{1}{2}\rho V_\infty^2 c},\ C_d = \frac{D'}{\frac{1}{2}\rho V_\infty^2 c},\ C_{m,o} = \frac{M'_{,o}}{\frac{1}{2}\rho V_\infty^2 c^2} \tag{2.56}$$

where the prime indicates that the force or moment is per unit span and the chord is the reference length in all cases in 2-D. Note that lower case subscripts will be used for two-dimensional coefficients to leave upper-case subscripts notation for wing, tail and complete configurations. Here, the moment coefficient is taken about point O, which in general will represent the leading edge of a profile or the nose of the airplane.

Other important quantities are:

- the lift slope $\frac{dC_l}{d\alpha}$
- the zero incidence lift coefficient $C_{l,0}$
- the moment slope $\frac{dC_{m,o}}{d\alpha}$
- the zero incidence moment coefficient $C_{m,o,0}$.

2.7.1 Center of Pressure—Aerodynamic Center

The center of pressure (c.p.) is the point about which the moment of the aerodynamic forces is zero.

The aerodynamics center (a.c.), also called neutral point, is the point about which the moment of the aerodynamic forces is independent of incidence.

2.7.2 Results for the Circular Cylinder

The reference length for the circular cylinder is the diameter $c = 2a$.

The pressure coefficient on the cylinder can be obtained from the velocity derived earlier

$$C_p(\theta) = 1 - \left(\frac{V(\theta)}{V_\infty}\right)^2 = 1 - \left(\frac{V_\theta}{U}\right)^2 = 1 - \left(2\sin\theta + \frac{\Gamma(\alpha)}{2\pi U a}\right)^2 \tag{2.57}$$

where $\Gamma(\alpha) = 4\pi U a \sin\alpha$. See Fig. 2.16 for the two cases $\alpha = 0$ and $\alpha = \frac{\pi}{2}$.

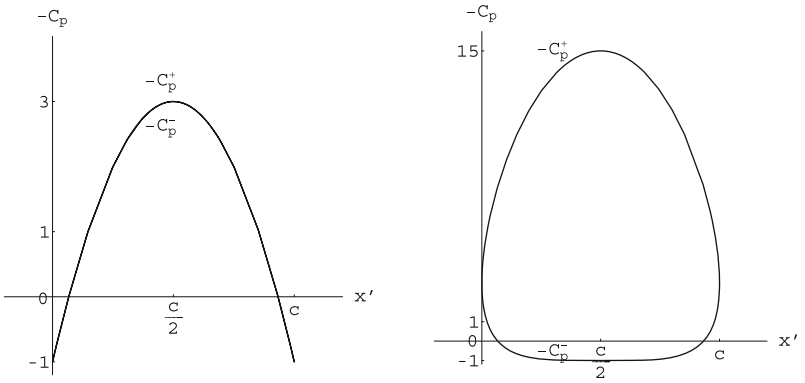

Fig. 2.16 Pressure coefficients for the cylinder, $\Gamma = 0$ (*left*), $\Gamma = 4\pi a$ (*right*)

The lift coefficient is

$$C_l(\alpha) = 4\pi \sin\alpha \tag{2.58}$$

This is a purely theoretical result, as real flow effects will dramatically change the flow field, compared to that shown in Fig. 2.9, even for small incidence angles. From the inviscid flow point of view, however, the cylinder at low incidence (near $\alpha = 0$) has a lift slope

$$\frac{dC_l}{d\alpha} = 4\pi \tag{2.59}$$

which is twice the result we will find in thin airfoil theory. The maximum lift that could be achieved theoretically with the small flap device is $C_{lmax} = 4\pi$, a very large number, when compared with high lift profiles, as we will see. This result corresponds to $\alpha = \frac{\pi}{2}$. See Fig. 2.17.

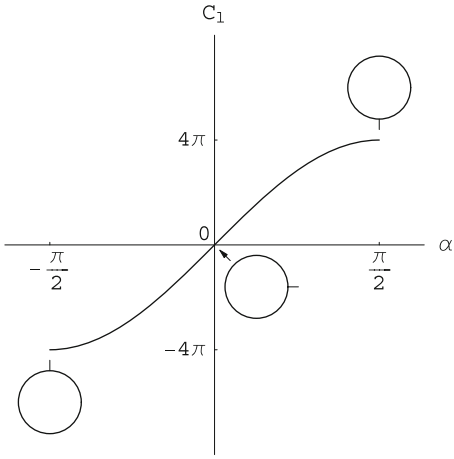

Fig. 2.17 Ideal cylinder-with-flap lift curve

The drag coefficient for the cylinder, as for all airfoils in inviscid, incompressible flow is (d'Alembert paradox)

$$C_d = 0 \tag{2.60}$$

In frictionless flow, the contact force between the fluid and the obstacle is normal to the surface. Hence, the center O of the cylinder is the center of pressure, i.e. $C_{m,o} = 0$ for all α's. This result indicates that O is also the aerodynamic center.

2.8 Special Cases of Joukowski Airfoils

2.8.1 The Ellipse at Zero Incidence

Consider the circle centered at the origin and of radius $b \geq a$ in the cylinder plane. Its image in the physical plane, through the Joukowski transformation, Eq. (2.39), is an ellipse centered at the origin, with main axis along Ox, from $-2a$ to $2a$ and with parametric representation

$$\begin{cases} x = \frac{b^2+a^2}{b}\cos\theta = \frac{c}{2}\cos\theta \\ z = \frac{b^2-a^2}{b}\sin\theta = \frac{e}{2}\sin\theta \end{cases} \tag{2.61}$$

where θ represents the polar angle in the cylinder plane. The ellipse has thickness e (small axis) and chord c (large axis). The potential function in the cylinder plane is

$$\Phi = U\left(r + \frac{b^2}{r}\right)\cos\theta \tag{2.62}$$

and the velocity components are

$$V_r = \frac{\partial\Phi}{\partial r} = U\left(1 - \frac{b^2}{r^2}\right)\cos\theta, \quad V_\theta = \frac{1}{r}\frac{\partial\Phi}{\partial\theta} = -U\left(1 + \frac{b^2}{r^2}\right)\sin\theta \tag{2.63}$$

On the surface of the cylinder, this reduces to

$$V_r = 0, \quad V_\theta = -2U\sin\theta \tag{2.64}$$

Using the chain rule

$$\begin{cases} \frac{\partial\Phi}{\partial r} = \frac{\partial\Phi}{\partial x}\frac{\partial x}{\partial r} + \frac{\partial\Phi}{\partial z}\frac{\partial z}{\partial r} \\ \frac{\partial\Phi}{\partial\theta} = \frac{\partial\Phi}{\partial x}\frac{\partial x}{\partial\theta} + \frac{\partial\Phi}{\partial z}\frac{\partial z}{\partial\theta} \end{cases} \tag{2.65}$$

and the Joukowski transformation

$$\begin{cases} x = \frac{r^2+a^2}{r}\cos\theta \\ z = \frac{r^2-a^2}{r}\sin\theta \end{cases} \tag{2.66}$$

the partial derivatives $\frac{\partial \Phi}{\partial x}$ and $\frac{\partial \Phi}{\partial z}$ can be solved for, on the ellipse as

$$\begin{cases} \frac{\partial \Phi}{\partial x} = 2U \frac{\left(1+\frac{a^2}{b^2}\right)\sin^2\theta}{\left(1+\frac{a^2}{b^2}\right)^2\sin^2\theta+\left(1-\frac{a^2}{b^2}\right)^2\cos^2\theta} \\ \frac{\partial \Phi}{\partial z} = -2U \frac{\left(1-\frac{a^2}{b^2}\right)\sin\theta\cos\theta}{\left(1+\frac{a^2}{b^2}\right)^2\sin^2\theta+\left(1-\frac{a^2}{b^2}\right)^2\cos^2\theta} \end{cases} \tag{2.67}$$

Upon eliminating θ in terms of x along the ellipse and a and b in terms of e and c, one obtains

$$\begin{cases} \frac{\partial \Phi}{\partial x} = U + u = U \frac{\left(1+\frac{e}{c}\right)\left(1-(\frac{2x}{c})^2\right)}{1-\left(\frac{2x}{c}\right)^2+(\frac{e}{c})^2\left(\frac{2x}{c}\right)^2} \\ \frac{\partial \Phi}{\partial z} = w = \pm U \frac{\left(1+\frac{e}{c}\right)\frac{e}{c}\frac{2x}{c}\sqrt{1-\left(\frac{2x}{c}\right)^2}}{1-\left(\frac{2x}{c}\right)^2+(\frac{e}{c})^2\left(\frac{2x}{c}\right)^2} \end{cases} \tag{2.68}$$

where the minus (plus) sign corresponds to the upper (lower) surface.

The above results reduce to the solutions for a circle ($\frac{e}{c} = 1$) and for the flat plate ($\frac{e}{c} = 0$). The surface speed on the ellipse is given by

$$\frac{V}{U} = \frac{\left(1+\frac{e}{c}\right)}{\sqrt{1+\left(\frac{e}{c}\right)^2\frac{\left(\frac{2x}{c}\right)^2}{1-\left(\frac{2x}{c}\right)^2}}} = \left(1+\frac{e}{c}-\frac{1}{2}\left(\frac{e}{c}\right)^2\frac{\left(\frac{2x}{c}\right)^2}{1-\left(\frac{2x}{c}\right)^2}+\cdots\right) \tag{2.69}$$

where the result has been expanded in terms of the small parameter $\frac{e}{c}$. The first order term in $\frac{e}{c}$ is constant (independent of x) and the same as the result of thin airfoil theory, as will be discussed in the next chapter. It is clear that any higher order term is singular at the leading edge (and trailing edge) for this blunt obstacle. The expansion is valid in the region $1-\left(\frac{2x}{c}\right)^2 > \frac{\left(\frac{e}{c}\right)^2}{1+\left(\frac{e}{c}\right)^2}$.

2.8.2 The Ellipse at Incidence

We proceed in the same way as before. The potential, with the flow coming at an angle α from the X-axis, reads

$$\Phi = U\left(r + \frac{b^2}{r}\right)\cos(\theta - \alpha) - \frac{\Gamma}{2\pi}(\theta - \alpha) \tag{2.70}$$

In this case, on the cylinder, the velocity components are

$$V_r = 0,\ \ V_\theta = -2U\sin(\theta - \alpha) - \frac{\Gamma}{2\pi b} \tag{2.71}$$

The circulation corresponding to a stagnation point at $\theta = 0$ is given by $\Gamma = 4Ub\sin\alpha$. On the surface of the ellipse, after some algebra, one finds

$$\begin{cases} \frac{\partial \Phi}{\partial x} = 2U\dfrac{\left(1+\frac{a^2}{b^2}\right)\left(\sin(\theta-\alpha)+\frac{\Gamma}{4Ub}\right)\sin\theta}{\left(1+\frac{a^2}{b^2}\right)^2\sin^2\theta+\left(1-\frac{a^2}{b^2}\right)^2\cos^2\theta} \\ \frac{\partial \Phi}{\partial z} = -2U\dfrac{\left(1-\frac{a^2}{b^2}\right)\left(\sin(\theta-\alpha)+\frac{\Gamma}{4Ub}\right)\cos\theta}{\left(1+\frac{a^2}{b^2}\right)^2\sin^2\theta+\left(1-\frac{a^2}{b^2}\right)^2\cos^2\theta} \end{cases} \tag{2.72}$$

Since the ellipse has a rounded trailing edge, there is no mechanism to control the circulation in inviscid flow and an ellipse at incidence will in general produce a flow with zero circulation. For $\Gamma = 0$ the two stagnation points are located at $\theta = \alpha$ and $\theta = \pi + \alpha$, see Fig. 2.18.

The pressure coefficient is given by

$$C_p(\theta) = 1 - \frac{4\sin^2(\theta - \alpha)}{\left(1 + \frac{a^2}{b^2}\right)^2\sin^2\theta + \left(1 - \frac{a^2}{b^2}\right)^2\cos^2\theta} \tag{2.73}$$

This is represented in Fig. 2.19 as $-C_p^+$ and $-C_p^-$ for the upper and lower surfaces, respectively.

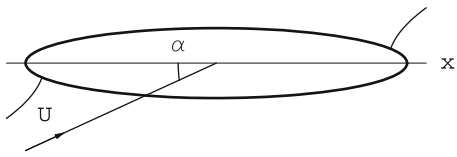

Fig. 2.18 Ellipse at 25° incidence ($\Gamma = 0$)

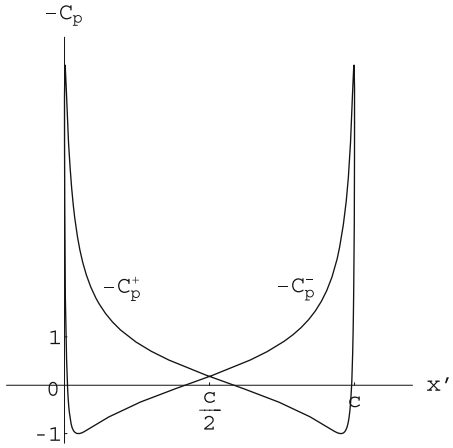

Fig. 2.19 Pressure coefficients for the ellipse at incidence ($\Gamma = 0$)

From anti-symmetry, the lift is zero. The moment however is not. It is obtained from

$$C_{m,o} = -\left(1 - \left(\frac{e}{c}\right)^2\right) \int_0^{2\pi} \frac{\sin^2(\theta - \alpha) \sin\theta \cos\theta}{\left(1 + \frac{a^2}{b^2}\right)^2 \sin^2\theta + \left(1 - \frac{a^2}{b^2}\right)^2 \cos^2\theta} d\theta \tag{2.74}$$

where O stands for the center of the ellipse, where the moment is calculated. After lengthy algebra, the result reads

$$C_{m,o} = \frac{\pi}{2}\left(1 - \left(\frac{e}{c}\right)^2\right) \sin\alpha \cos\alpha \tag{2.75}$$

Again, the results for the circle and the flat plate are obtained for $\frac{e}{c} = 1$ and $\frac{e}{c} = 0$, respectively.

In order to force the flow to stagnate at $\theta = 0$, a small flap can be added at the trailing edge of the ellipse. In this case, the circulation corresponding to a stagnation point at $\theta = 0$ is given by $\Gamma = 4\pi U b \sin\alpha$ and the velocity components can be written as

$$\begin{cases} \frac{\partial \Phi}{\partial x} = 4U \frac{\left(1+\frac{a^2}{b^2}\right) \sin\frac{\theta}{2} \cos(\frac{\theta}{2} - \alpha) \sin\theta}{\left(1+\frac{a^2}{b^2}\right)^2 \sin^2\theta + \left(1-\frac{a^2}{b^2}\right)^2 \cos^2\theta} \\ \frac{\partial \Phi}{\partial z} = -4U \frac{\left(1-\frac{a^2}{b^2}\right) \sin\frac{\theta}{2} \cos(\frac{\theta}{2} - \alpha) \cos\theta}{\left(1+\frac{a^2}{b^2}\right)^2 \sin^2\theta + \left(1-\frac{a^2}{b^2}\right)^2 \cos^2\theta} \end{cases} \tag{2.76}$$

The two stagnation points are now located at $\theta = 0$ and $\theta = \pi + 2\alpha$. The corresponding flow is sketched in Fig. 2.20.

The surface pressure distribution for the ellipse with a small flap is shown in Fig. 2.21.

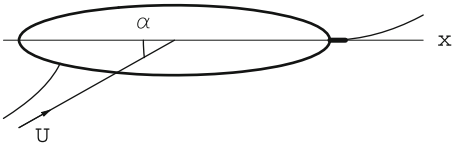

Fig. 2.20 Flow past an ellipse with a small flap at the trailing edge

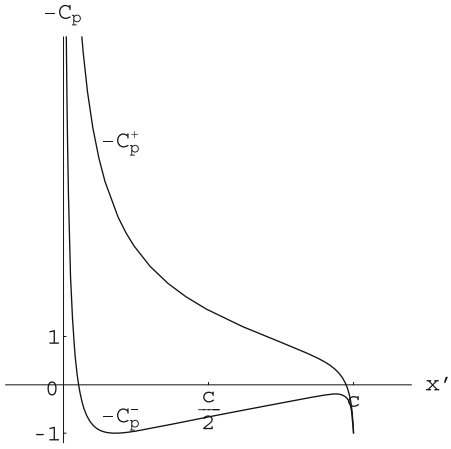

Fig. 2.21 Pressure distribution on the ellipse with small flap at the trailing edge

The lift coefficient is given by the Kutta-Joukowski lift theorem

$$C_l = \frac{2\Gamma}{Uc} \tag{2.77}$$

where $c = 2(b^2 + a^2)/b$. Substituting the value of the circulation gives

$$C_l = 4\pi \frac{b^2}{b^2 + a^2} \sin\alpha = 2\pi \left(1 + \frac{e}{c}\right) \sin\alpha \tag{2.78}$$

The results for the cylinder and the flat plate are obtained for $e/c = 1$ and $e/c = 0$, respectively. In small perturbation theory, the term e/c can be neglected as a second-order term when multiplied by $sin\alpha \simeq \alpha$.

2.8.3 The Flat Plate at Incidence

For this case, Joukowski transformation has $\epsilon = \delta = 0$. The flat plate is mapped into a circle with its center at the origin in the (X, Z)-plane, Fig. 2.22. The mapping can be interpreted as a conformal transformation from the cylinder plane to the physical plane such that $x = \Phi/U$, $z = \Psi/U$, where Φ and Ψ are the velocity potential and stream function of the flow past a circular cylinder without circulation. Indeed, Eqs. (2.30) and (2.31) written in terms of X and Z read

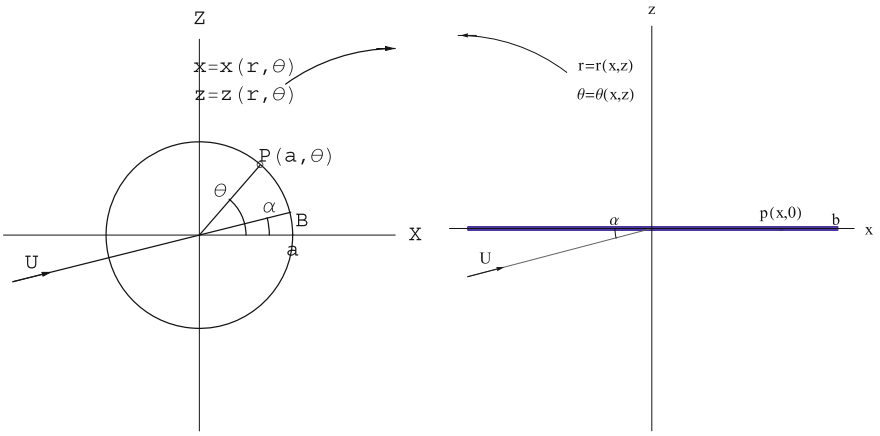

Fig. 2.22 Flat plate transformation

$$x = \frac{\Phi}{U} = \left(r + \frac{a^2}{r}\right)\cos\theta = X\left(1 + \frac{a^2}{X^2 + Z^2}\right) \tag{2.79}$$

$$z = \frac{\Psi}{U} = \left(r - \frac{a^2}{r}\right)\sin\theta = Z\left(1 - \frac{a^2}{X^2 + Z^2}\right) \tag{2.80}$$

In this transformation, the cylinder of radius a centered at the origin, which corresponds to the stagnation streamline $\Psi = 0$, is mapped onto the x-axis ($z = 0$), in the interval $[-2a, 2a]$.

This case corresponds to $b = a = \frac{c}{4}$ in Sects. 2.8.1 and 2.8.2, and the results derived previously can be used.

In the mapping, the flat plate parametric representation is given by

$$x = 2a\cos\theta = \frac{c}{2}\cos\theta, \;\; z = 0 \tag{2.81}$$

and the velocity components in the physical plane are

$$\begin{cases} \frac{\partial \Phi}{\partial x} = 2U\frac{\left(\sin(\theta-\alpha)+\frac{\Gamma}{4\pi a}\right)}{\sin\theta} \\ \frac{\partial \Phi}{\partial z} = 0 \end{cases} \tag{2.82}$$

Forcing the circulation to be zero yields an anti-symmetric flow that does not satisfy the Kutta-Joukowski condition, Fig. 2.23. The lift is zero, but the moment coefficient about the mid-plate reduces to

$$C_{m,o} = \frac{\pi}{2}\sin\alpha\cos\alpha \tag{2.83}$$

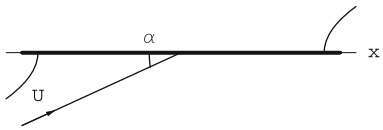

Fig. 2.23 Flat plate at 25° incidence ($\Gamma = 0$)

Making use of the mapping, the velocity on the flat plate now reads

$$\begin{cases} \frac{\partial \Phi}{\partial x} = 2U\left(\cos\alpha \mp \sin\alpha \frac{\frac{2x}{c}}{\sqrt{1-(\frac{2x}{c})^2}}\right) \\ \frac{\partial \Phi}{\partial z} = 0 \end{cases} \tag{2.84}$$

where the minus (plus) sign corresponds to the upper (lower) surface. The stagnation points are at $x = \pm\frac{c}{2}\cos\alpha$, $z = 0$.

When the Kutta-Joukowski condition is applied, the velocity on the flat plate becomes

$$\frac{\partial \Phi}{\partial x} = U\frac{\cos\left(\frac{\theta}{2} - \alpha\right)}{\cos\frac{\theta}{2}}, \quad \frac{\partial \Phi}{\partial z} = 0 \tag{2.85}$$

The streamline in this case leaves the trailing edge "smoothly", Fig. 2.24.

Note that the velocity is infinite at $\theta = \pi$ (leading edge) in all cases except for $\alpha = 0$. The stagnation point corresponds to $\theta = \pi + 2\alpha$, i.e. $x = -\frac{c}{2}cos2\alpha$. It is also worthy to note that the exact solution is consistent with the thin airfoil theory result that will be derived in the next chapter, since the flat plate is the ultimate thin airfoil, having zero thickness and zero camber. Another assumption that will be made is that of small α. If we map the flat plate to the segment $[0, c]$ with $x' = \frac{c}{2}\left(1 + \frac{x}{2a}\right)$ the horizontal velocity component becomes

$$\frac{\partial \Phi}{\partial x} = U\left(cos\alpha \pm sin\alpha\sqrt{\frac{c-x'}{x'}}\right) \simeq U\left(1 \pm \alpha\sqrt{\frac{c-x'}{x'}}\right) \tag{2.86}$$

The plus (minus) sign corresponds to the upper (lower) surface. This last result is the thin airfoil result with a perturbation u above and below the plate that is symmetric about the x'-axis.

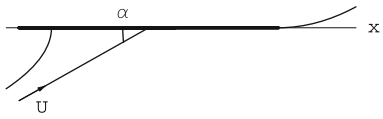

Fig. 2.24 Flat plate at 25° incidence ($\Gamma = 4\pi asin\alpha$)

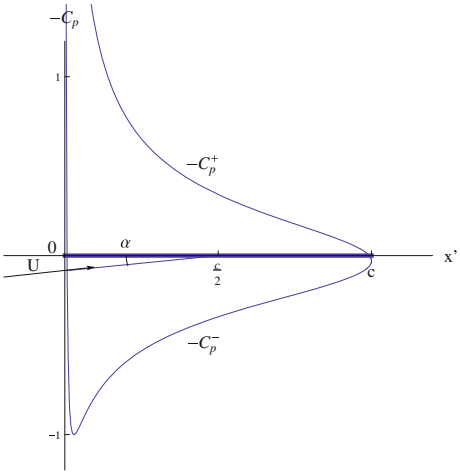

Fig. 2.25 Pressure coefficient along the plate at $\alpha = 10°$

The pressure coefficient is given by

$$C_p(\theta) = 1 - \left(\frac{cos(\frac{\theta}{2} - \alpha)}{cos\frac{\theta}{2}} \right)^2 \tag{2.87}$$

The result for $-C_p$ is displayed in Fig. 2.25. It is not symmetric w.r.t. the Ox'-axis. If we anticipate again on thin airfoil theory, the linearized C_p will be symmetric, i.e. $C_p^- = -C_p^+$.

The lift coefficient is obtained from the Kutta-Joukowski lift theorem

$$C_l = \frac{\rho U \Gamma}{\frac{1}{2}\rho U^2 4a} = 2\pi sin\alpha \tag{2.88}$$

It is interesting, however, to consider the integration of the pressure along the flat plate directly. The result is expected to be normal to the plate, i.e. in the z-direction. Indeed, integrating in θ the elementary forces due to pressure around the plate yields the pressure contribution $\mathbf{F'_p} = (0, F'_p)$, where

$$F'_p = 4\pi\rho U^2 a sin\alpha \, cos\alpha \tag{2.89}$$

On the other hand, the lift per unit span, as given by the Kutta-Joukowski theorem is

$$L' = 4\pi\rho U^2 a sin\alpha \tag{2.90}$$

acting in a direction perpendicular to the incoming velocity vector as $\mathbf{L'} = (-L' sin\alpha, L' cos\alpha)$. The difference between these results is due to a horizontal suction force $\mathbf{F'_s} = (F'_s, 0)$ acting at the leading edge, in the direction of the negative x-axis, that is

due to the leading edge singularity. This missing component, parallel to the camber line and of magnitude

$$F_s' = -4\pi\rho U^2 a sin^2\alpha \tag{2.91}$$

points to the fact that integration of pressure does not capture the localized force that exists at a sharp leading edge.

The moment w.r.t. the leading edge is the sum of elementary moments

$$dM_{,o} = -\frac{1}{2}\rho U^2 C_p(\theta)(x(\theta) + 2a)dx(\theta) \tag{2.92}$$

Here, O stands for the leading edge. The moment is given by

$$M_{,o} = 2\rho U^2 a^2 \int_0^{2\pi} \left(1 - \left(\frac{cos(\frac{\theta}{2} - \alpha)}{cos\frac{\theta}{2}}\right)^2\right)(1 + cos\theta)sin\theta \; d\theta \tag{2.93}$$

Some simplifications occur when the half-angle $\frac{\theta}{2}$ is used. The result is

$$M_{,o} = -2\pi\rho U^2 a^2 sin2\alpha \tag{2.94}$$

and the moment coefficient reads

$$C_{m,o} = -\frac{\pi}{4} sin2\alpha \tag{2.95}$$

The moment of the aerodynamic forces can be calculated at an arbitrary point D along the x'-axis as $C_{m,D} = C_{m,o} + \frac{x_D'}{c} C_l$. The center of pressure satisfies $C_{m,c.p.} = 0$, i.e.

$$\frac{x_{c.p.}'}{c} = -\frac{C_{m,o}}{C_l} = \frac{1}{4} cos\alpha \simeq \frac{1}{4} \tag{2.96}$$

For small values of α, the center of pressure for the flat plate is located at the quarter-chord.

Taking the derivative w.r.t. α of the same general formula for the moment at point D and now setting the result to zero, gives the aerodynamics center

$$\frac{\partial C_{m,D}}{\partial\alpha} = -\frac{\pi}{2} cos2\alpha + \frac{x_D'}{c} 2\pi cos\alpha = 0 \tag{2.97}$$

For small values of α one obtains the small perturbation result derived in the next chapter

$$\frac{x_{a.c.}'}{c} = \frac{1}{4} \tag{2.98}$$

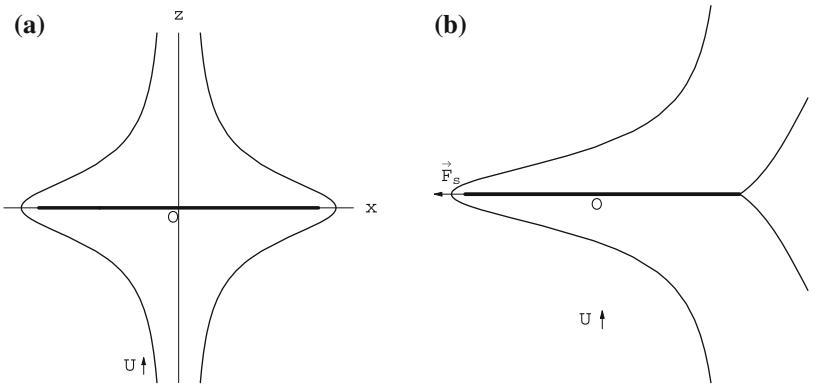

Fig. 2.26 Flat plate perpendicular to incoming flow **a** with zero circulation and **b** with trailing edge that satisfies the K-J condition, and suction force

To close this section, the limiting case of the flow coming perpendicular to the plate ($\alpha = 90°$) is considered, with the plate having zero circulation or satisfying the Kutta-Joukowski condition. The two results are shown in Fig. 2.26.

In Fig. 2.26a, the flow is perfectly symmetric about the mid-plate and the net resulting force and moments are zero. Again, this is an idealized flow representation and viscosity will radically change the picture by having separation at the sharp edges of the plate. The same can be said of Fig. 2.26b in terms of realism of the picture, but it is intriguing to observe that there is circulation, hence lift, and the force is not perpendicular to the flat plate, but aligned with the plate and to the left. The occurrence of such a force, again a suction force, will be discussed in more details in the next chapter.

2.8.4 Circular Arc

For this case, $\epsilon = 0$ and $\delta > 0$. The polar coordinates are centered at $(0, \delta)$. The potential function reads

$$\Phi = 2Ua' \cos(\theta - \alpha) - \frac{\Gamma}{2\pi}(\theta - \alpha) \tag{2.99}$$

where $a'^2 = a^2 + \delta^2$. The azimuthal component of velocity on the cylinder is

$$V_\theta = -2U \sin(\theta - \alpha) - \frac{\Gamma}{2\pi a'} \tag{2.100}$$

The circulation, that places the stagnation point at $(0, a)$ is

$$\Gamma = 4\pi U\,(a\sin\alpha + \delta\cos\alpha) \tag{2.101}$$

and the lift coefficient as given by the Kutta-Joukowski lift theorem

$$C_l = 2\pi\left(\sin\alpha + \frac{\delta}{a}\cos\alpha\right) \tag{2.102}$$

The most interesting situation for this airfoil corresponds to $\alpha = 0$ where a symmetry w.r.t. the z-axis (and Z-axis) is obtained. In this case, the surface velocity reduces to a simple expression

$$\frac{V}{U} = \frac{a^2 + 2\delta\sin\theta\sqrt{a^2 + (\delta\sin\theta)^2}}{a^2 + \delta^2} \tag{2.103}$$

The pressure coefficients are shown in Fig. 2.27 for $\alpha = 0$, $\frac{d}{c} = 0.1$ and $\frac{d}{c} = 0.2$.

A consequence of symmetry is that the leading edge, as the trailing edge, satisfies a Kutta-Joukowski condition. This is only possible for $\alpha = 0$. The leading edge is "adapted". $\alpha = 0$ is the ideal angle of attack for the circular arc. The lift coefficient in this case is $C_l = 2\pi\frac{\delta}{a}$. The lift per unit span

$$L' = 4\pi\rho U^2\delta = 2\pi\rho U^2 d \tag{2.104}$$

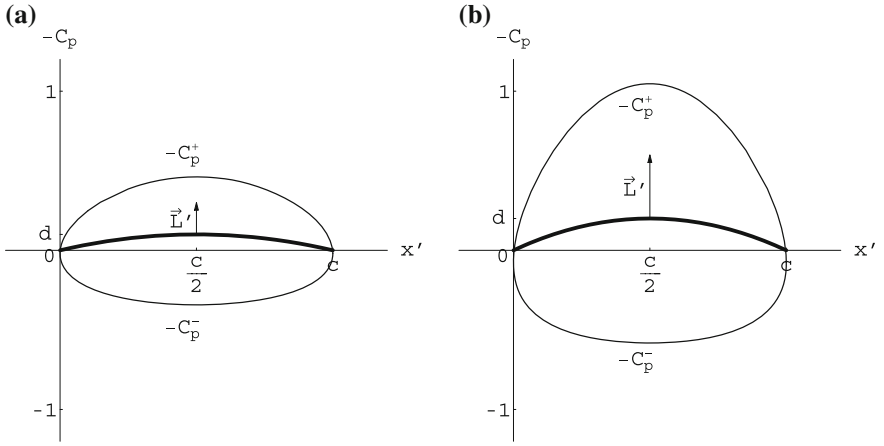

Fig. 2.27 C_p distributions for the circular arc at $\alpha = 0$: **a** $\frac{d}{c} = 0.1$, **b** $\frac{d}{c} = 0.2$

only depends on d, where $d = 2\delta$ represents the height of the circular arc in the physical plane (the chord is $c = 4a$). This result was first obtained by Kutta in 1902. The center of pressure is at the center of the arc, i.e.

$$\frac{x'_{c.p.}}{c} = \frac{1}{2} \tag{2.105}$$

2.8.5 Joukowski Airfoil at Incidence

The same result for the potential function is obtained in this case with $\epsilon \geq 0$ and $\delta \geq 0$

$$\Phi = 2Ua' \cos(\theta - \alpha) - \frac{\Gamma}{2\pi}(\theta - \alpha) \tag{2.106}$$

where now $a'^2 = (a + \epsilon)^2 + \delta^2$, with the following formula for the circulation that enforces the Kutta-Joukowski condition

$$\Gamma = 4\pi U \left((a + \epsilon) \sin\alpha + \delta \cos\alpha\right) \tag{2.107}$$

and lift coefficient

$$C_l = 2\pi \left(\left(1 + \frac{\epsilon}{a}\right) \sin\alpha + \frac{\delta}{a} \cos\alpha\right) \tag{2.108}$$

The exact solution is quite complicated and is best calculated numerically. However, assuming small values for thickness and camber, i.e. $\frac{\epsilon}{a} \ll 1$ and $\frac{\delta}{a} \ll 1$, the formula can be linearized to give the x-component of velocity as

$$\frac{\partial \Phi}{\partial x} = U \frac{\cos\left(\frac{\theta}{2} - \alpha\right)}{\cos\left(\frac{\theta}{2}\right)} \left(1 - 2\left\{\frac{\epsilon}{a} \cos\theta - \frac{\delta}{a} \sin\theta\right\}\right. \tag{2.109}$$

$$\left. + \left\{\frac{\epsilon}{a} \cos\alpha - \frac{\delta}{a} \sin\alpha\right\} \frac{\cos\left(\frac{\theta}{2}\right)}{\cos\left(\frac{\theta}{2} - \alpha\right)}\right) \tag{2.110}$$

This formula holds for all values of incidence, $|\alpha| \leq \frac{\pi}{2}$. For small values of α the small disturbance result is recovered. For example, for $\alpha = \delta = 0$ and $\frac{\epsilon}{a} = 0.077$ corresponding to a 10 % thick symmetric Joukowski airfoil, the pressure coefficient at zero incidence is shown in Fig. 2.28.

The thin airfoil solution is a straight line, since the perturbation velocity in x' is linear

$$U + u(x') = U\left(1 + \frac{4}{3\sqrt{3}} \frac{e}{c}\left(3 - 4\frac{x'}{c}\right)\right) \tag{2.111}$$

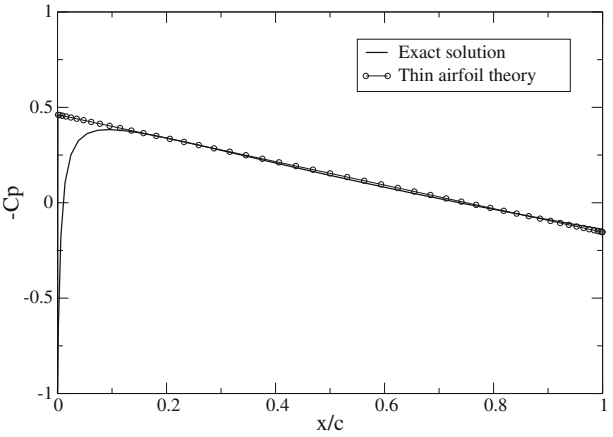

Fig. 2.28 Comparison of exact and numerical (small disturbance) C_p distributions

To find the solution in the physical plane and in particular the surface velocity for arbitrary Joukowski airfoils, the values of the potential function at certain points on the circle, image of the profile, are first calculated. The same values are assigned to the corresponding points on the airfoil which can be found from the transformation formulae. The surface velocity can be evaluated numerically as

$$V = \frac{\Delta\Phi}{\Delta s} \tag{2.112}$$

where $\Delta\Phi$ is the difference between the values of Φ at the two close points on the surface and Δs is the length of the airfoil segment between these two points. The surface pressure distribution is readily obtained from Bernoulli's law, i.e.

$$C_p = 1 - \left(\frac{V}{U}\right)^2 \tag{2.113}$$

2.9 Summary of Chapter 2

In this Chapter, mathematical solutions are found analytically for a theoretical model of steady, two-dimensional, inviscid, incompressible, adiabatic flow with uniform upstream conditions. This flow has no vorticity. The governing first order partial differential equations (Cauchy/Riemann system) for the velocity components are linear, representing conservation of mass and the irrotationality condition. The pressure is decoupled and is obtained from Bernoulli's law.

The Cauchy/Riemann system can be replaced by a single potential or stream-function equation which satisfies Laplace equation. The uniform flow is a trivial

solution of these equations. Other fundamental solutions are found (i.e. source/sink and potential vortex) and more general solutions are constructed via superposition, for example doublet and half-body flows.

The solution for the flow over a circular cylinder is of particular interest. The boundary conditions are the tangency condition at the solid surface and uniform flow in the far field. From symmetry, the cylinder has zero lift and zero drag. The latter result is referred to d'Alembert Paradox. In the real flow, there is drag due to friction and due to the difference in pressure on the front and the back of the cylinder because of separation. However, this mathematical solution is useful since it provides the pressure distributions over thin bodies at small angle of attack via mapping techniques. For example, the Joukowski transformation provides analytical solutions for a family of symmetric shapes. In such cases, the flow is attached and the viscous effects are confined to the thin boundary layers, hence the mathematical model of inviscid flow yields a reasonable approximation.

A more interesting case is the flow with lift. Flow asymmetry is necessary to generate lift. One can think of a rotating cylinder. In the real flow, the effect of the rotation of the cylinder is transmitted through a viscous layer, augmenting the velocity on one side and retarding it on the other, thus creating a circulatory flow and lift. The inviscid flow model however, admits a slip velocity at the surface and has no mechanism to control the asymmetry other than adding a small flap to force flow stagnation at a specified point on the surface of the cylinder. The mathematical solution is obtained as uniform flow plus a doublet and a potential vortex. The doublet strength is determined to satisfy the tangency condition at the cylinder surface. In general the mathematical solution is not realistic since there is flow separation (unless the cylinder rotates so fast that the boundary layer is confined to a thin annulus attached to the surface). Through the Joukowski transformation however, the solution can be mapped to a flow over a lifting airfoil. To obtain a solution consistent with the experimental results, at least for small angles of attack when the flow is attached and the viscous effects are confined to thin boundary layers, the circulation in the mathematical model is chosen such that the flow leaves the trailing edge smoothly, in a direction bisecting the trailing edge angle. This celebrated Kutta-Joukowski condition renders the mathematical solution unique by choosing the most physically relevant solution which has no flow around the trailing edge, since in a real flow, the viscous effects will not allow such a behavior.

Once the vortex strength is determined, the lift is calculated via the Kutta-Joukowski lift theorem which is based on momentum balance. The same result can be obtained by integrating the surface pressure.

The Kutta-Joukowski transformation has allowed us to obtain exact solutions for the flow past ellipses, flat plates and Joukowski airfoils. The circles in the cylinder plane and their images in the physical plane are shown for example in Fig. 2.29.

Finally, the main formulae in this chapter are the Kutta-Joukowski lift theorem result $L' = \rho U \Gamma$ and the relation between the strength of the potential vortex and the position of the stagnation points on the cylinder. Through the Joukowski transformation, these formulae reveal the dependence of the lift on the angle of attack for a family of airfoils.

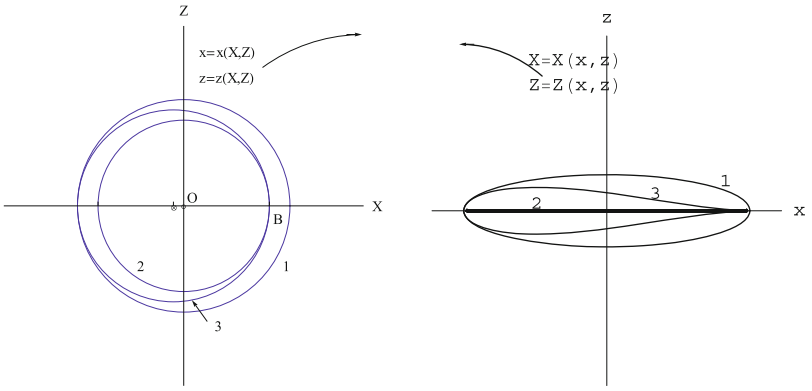

Fig. 2.29 Circles *1*, *2* and *3* in the cylinder plane and their images: *1* ellipse, *2* flat plate, *3* Joukowski profile

In the next chapter, thin airfoil theory is introduced. The same results can be obtained numerically, using for example the method of singularities.

More accurate analyses, where the viscous effects in the boundary layer are fully accounted for, are presented later. Also, compressibility and three-dimensional effects are dealt with in separate chapters.

2.10 Problems

2.10.1

A 2-D model for tornadoes can be described as a core cylinder of fluid with solid body rotation and a potential vortex flow outside the core. Plot the velocity distribution and streamlines. Plot the lines of constant potentials where they exist. What is Bernoulli's law for such a flow? Calculate the pressure distribution and in particular the pressure at the center (Hint: use normal momentum equation to calculate the pressure in the core).

2.10.2

A 2-D model for hurricanes can be described by a potential vortex and a source for the flow outside the core. Show that the streamlines are spirals. Find the velocity and pressure distributions.

2.10.3

Derive the formula for velocity distributions due to a doublet using summation of velocity vectors of a sink and a source of strength Q and a distance $2a$ apart, in the limit of $a \to 0$ and $Q \to \infty$, such that $aQ = D$.

2.10.4

Show that the velocity due to a doublet with its axis in the x-direction is the derivative with respect to x of the velocity field due to a source.

2.10.5

Show that a doublet can be produced by a pair of counter rotating potential vortices of strength Γ and $-\Gamma$ at a distance $2a$, along the z-axis, in the limit $a \to 0$ and $\Gamma \to \infty$, such that $a\Gamma$ is finite (Fig. 2.30).

2.10.6

Show that the velocity due to a doublet with its axis in the x-direction is the derivative w.r.t. z of the velocity field due to a potential vortex.

2.10.7

Obtain the velocity and pressure distributions around a Rankine body described by the closed streamline due to a source and a sink of equal strength and at a distance $2a$ apart in a uniform stream.

2.10.8

Obtain the velocity and pressure distributions around a Kelvin body described by the closed streamline due to a pair of potential vortices of equal strength and opposite direction in a uniform stream, perpendicular to their axis.

2.10.9

Show that the Joukowski transformation with $\epsilon = \delta = 0$, maps a circle to a flat plate with $c = 4a$, hence for a flat plate at incidence produces a lift $C_l = 2\pi \sin\alpha$. What is the drag coefficient C_d? Explain d'Alembert paradox, considering that the pressure acting normal to the flat plate will produce a force normal to the plate and not normal to the flow direction!

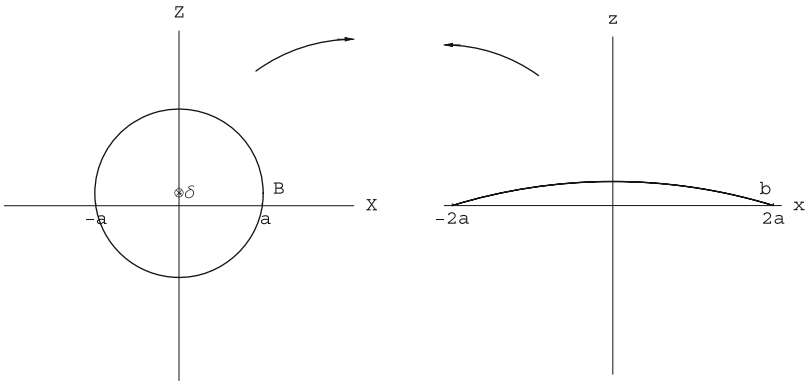

Fig. 2.30 Problem 2.10.10

2.10.10

Show that the Joukowski transformation with $\epsilon = 0$ and $0 < \delta \ll 1$ maps a circle to a shallow circular arc as in Fig. 2.27. Find the pressure distribution over the circular arc and calculate C_l and C_d. Where is the center of pressure? Where is the aerodynamic center?

2.10.11

Consider an ellipse at incidence. Show that the lift is zero. Consider next an ellipse with a small flap at the trailing edge. Find the lift (Hint: use Joukowski transformation).

Construct a symmetric airfoil with a blunt leading edge and a sharp trailing edge (Hint: use a parabola or a circle for the nose and a cubic or a quartic for the rest of the airfoil). Plot the airfoil shape.

Reference

1. White, F.M.: Fluid Mechanics, 7th edn. McGraw Hill, New York (2009)

http://www.springer.com/978-94-017-9824-2

Theoretical and Applied Aerodynamics
and Related Numerical Methods
Chattot, J.-J.; Hafez, M.
2015, XXI, 620 p. 325 illus., 141 illus. in color.,
Hardcover
ISBN: 978-94-017-9824-2